Optimising Conformational Effects on Thermally Activated Delayed Fluorescence

Alessandro Landi,[a*] Daniele Padula[b†]

[a]*Dipartimento di Chimica e Biologia Adolfo Zambelli, Università di Salerno, Via Giovanni Paolo II, I-84084 Fisciano (SA), Italy*
[b]*Dipartimento di Biotecnologie, Chimica e Farmacia, Università di Siena, Via A. Moro 2, 53100 Siena, Italy*

Supporting Information

---
[*]To whom correspondence should be addressed. Email: alelandi1@unisa.it
[†]To whom correspondence should be addressed. Email: daniele.padula@unisi.it

Contents

List of Figures

List of Tables

We provide optimised geometries, and the implementation of the kinetic model at this public GitHub repository https://github.com/dpadula85/PareTADF.

S1 Fermi's Golden Rule

We evaluated rate constants by first order time-dependent perturbation theory, Fermi's Golden Rule (FGR), whose general form is reported in Eq. 1 in the main text.

As discussed in the main text, FGR final form depends on the process involved,[1–3] i.e. non-radiative transition, spontaneous emission or absorption.

In the cases of interest here, the $S_1{\rightarrow}T_1$ transition is a non radiative transition, and the Fermi Golden Rule assumes the form:

$$k_{ij,nr} = \frac{2\pi}{\hbar}|SOC_{ij}|^2 F(\Delta E_{ij}, T). \tag{S1}$$

where SOC_{ij} is the spin-orbit coupling element, $F(\Delta E_{ij}, T)$ is the Franck-Condon weighted density of states (FCWD) and ΔE_{ij} is the energy difference between the two electronic states.

On the other hand, when dealing with a spontaneous emission,[1,3–6] the FGR rates expression is

$$k_{ij,em} = \int_{-\infty}^{+\infty} \frac{64\pi^4\nu^3}{3hc}|\mu_{ij}|^2 F(h\nu, T)d(h\hat{\jmath}). \tag{S2}$$

where μ is the dipole moment operator for the $S_1{\rightarrow}S_0$ transition and the integration goes over the whole frequency spectrum.

In both cases, the FCWD $F(\Delta E_{ab}, T)$ is defined as:

$$F(\Delta E_{ab}, T) = \frac{1}{Z}\sum_{v_a, v_b} e^{-\beta E_{v_i}}|\langle v_a|v_b\rangle|^2 \delta\big(E_{v_b} - E_{v_a} - \Delta E\big) \tag{S3}$$

where $\langle v_a|v_b\rangle$ is the Franck-Condon integral, Z is the vibrational partition function of the initial electronic state, $\beta = 1/(k_B T)$, and the sum runs over all vibrational states of $|a\rangle$ and $|b\rangle$.

Here, we have adopted for its evaluation the generating function (GF) approach,[1,2] which, in the framework of harmonic approximation for nuclear motion, allows to compute $F(\Delta E_{ab}, T)$ considering the whole set of the molecular normal modes of both initial and final states, taking into account the effects due to both changes of the equilibrium positions and of vibrational frequencies, as well as the effects due to normal mode mixing. The GF approach allows to handle the infinite summations appearing in Eq. S3 exploiting the integral representation of Dirac's delta function and Duschinsky's normal mode transformation:[7]

$$\mathbf{Q}_a = \mathbf{J}\mathbf{Q}_b + \mathbf{K} \tag{S4}$$

where $\mathbf{J}$ and $\mathbf{K}$ are the rotation matrix and the equilibrium displacement vector, respectively, while $\mathbf{Q}_a$ and $\mathbf{Q}_b$ are the normal coordinates of the electronic states $|a\rangle$ and $|b\rangle$.

We obtained Franck-Condon weighted densities of states (FCWDs) using a development version of the MolFC package,[8] using (TD-)DFT/B3LYP-D3/6-31G(d) for geometry optimisations and normal modes analyses. We adopted the curvilinear coordinate representation of normal modes, to prevent that large displacements of an angular coordinate could reflect into large shifts from the equilibrium positions of the involved bond distances. Such unphysical effect is unavoidable when using rectilinear coordinates and requires the use of high order anharmonic potentials for its correction.[9,10]

Finally, the rates of endoergonic processes (such as rISC) are obtained from those of the reverse processes using the principle of detailed balance:[11,12]

$$k_{ba} = k_{ab} \times \exp\left(-\frac{\Delta E_{ba}}{k_{\mathrm{B}}T}\right), \tag{S5}$$

where k_{ab} is evaluated at ΔE_{ab}, k_{B} is the Boltzmann constant and T is the temperature.

S2   Franck-Condon Weighted Densities of States

Fig. S1: Franck-Condon weighted densities of states at $T = 298$ K as a function of the energy difference from the initial and the final states for the S1→T1 transition. TOP: tn4t. Bottom: acpm.
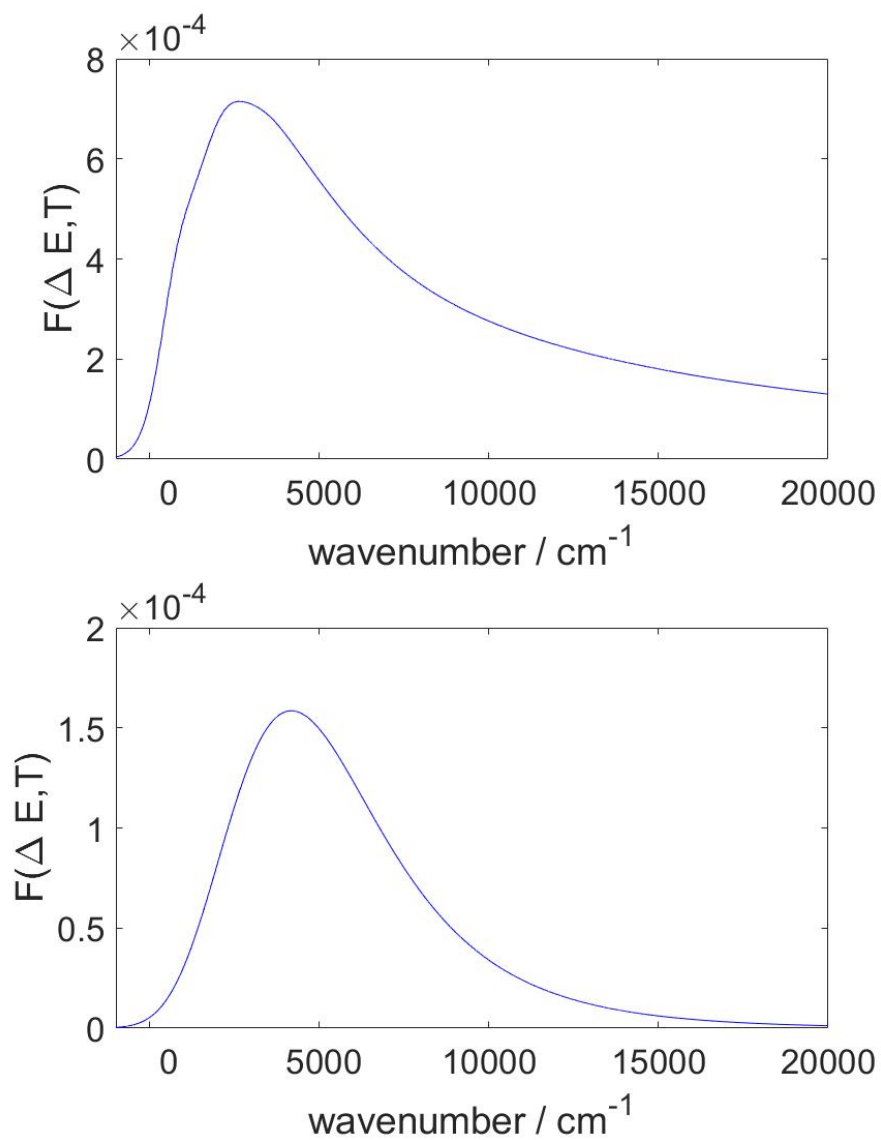
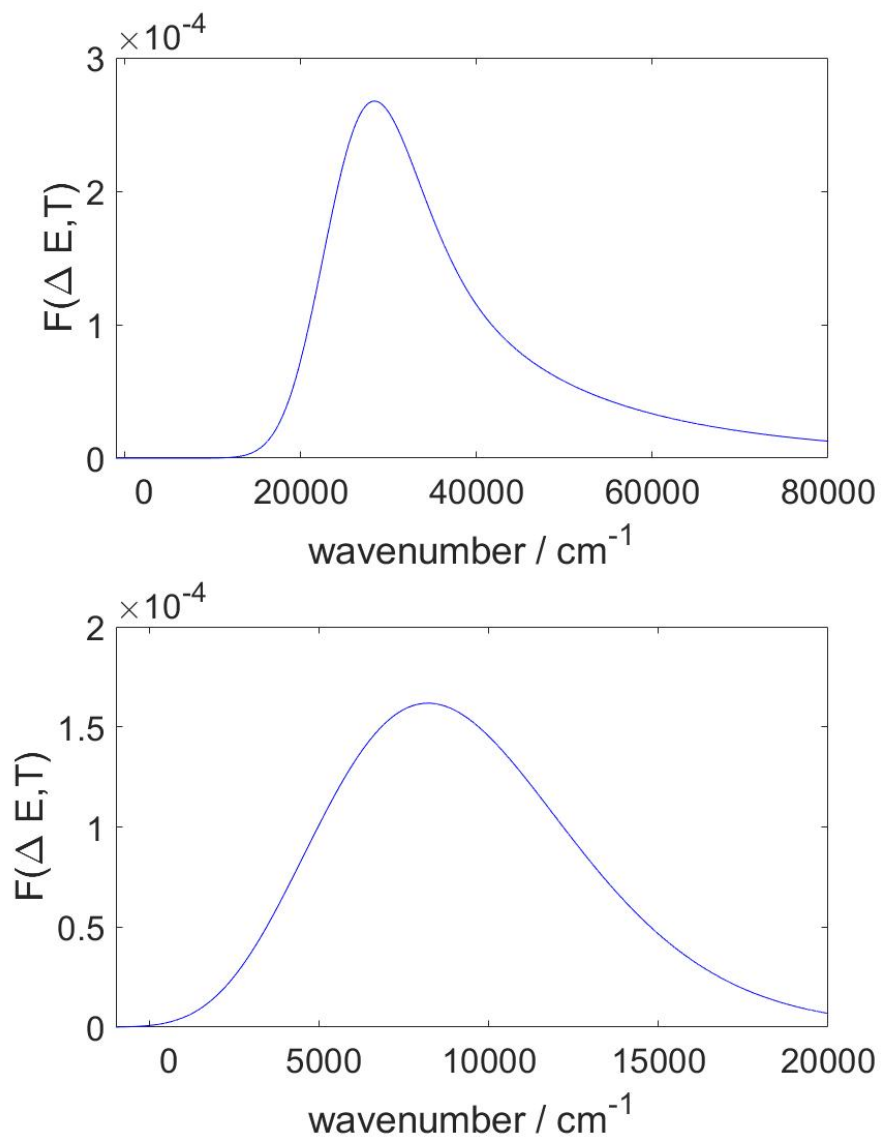**Fig. S2:** Franck-Condon weighted densities of states at $T = 298$ K as a function of the energy difference from the initial and the final states for the S1→S0 transition. TOP: tn4t. Bottom: acpm.

S3 Kinetic Model

Dye	k_{em} / s^{-1}	k_{ISC} / s^{-1}	k_{rISC} / s^{-1}	k_{nr} / s^{-1}
TN4T min	2.1×10^9	9.7×10^7	3.5×10^2	3.2×10^8
TN4T opt ratio	1.9×10^8	1.1×10^6	1.0×10^6	2.9×10^7
ACPM min	6.2×10^3	6.9×10^3	4.6×10^3	1.2×10^3
ACPM opt ratio	1.0×10^6	1.0×10^6	8.7×10^4	2.0×10^5

Table S1: Rates of the processes considered for the integration of Eq. 4.
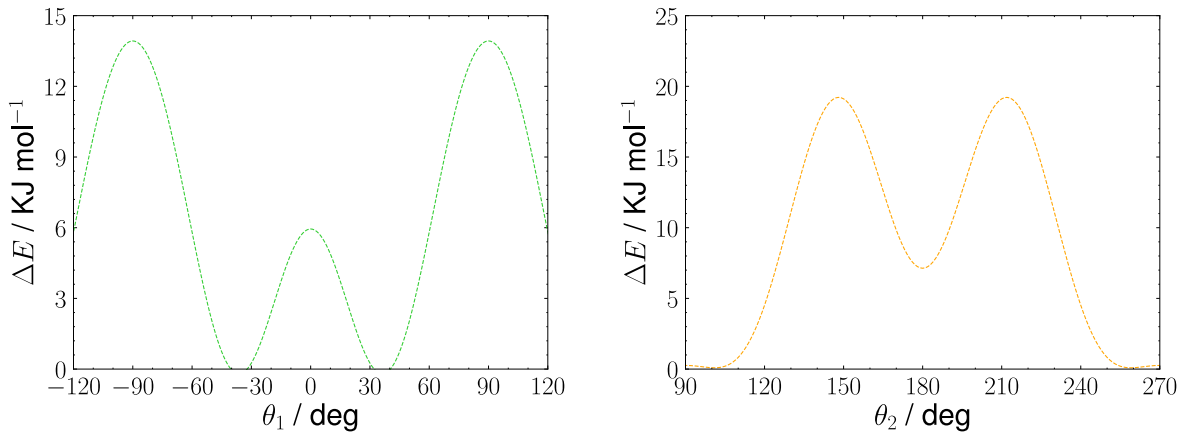
S4 PES Scans

Fig. S3: Fit of QM relaxed scans on S$_0$ PES along the torsional coordinates highlighted in Fig. 4 for TN4T (left) and ACPM (right) derivatives.
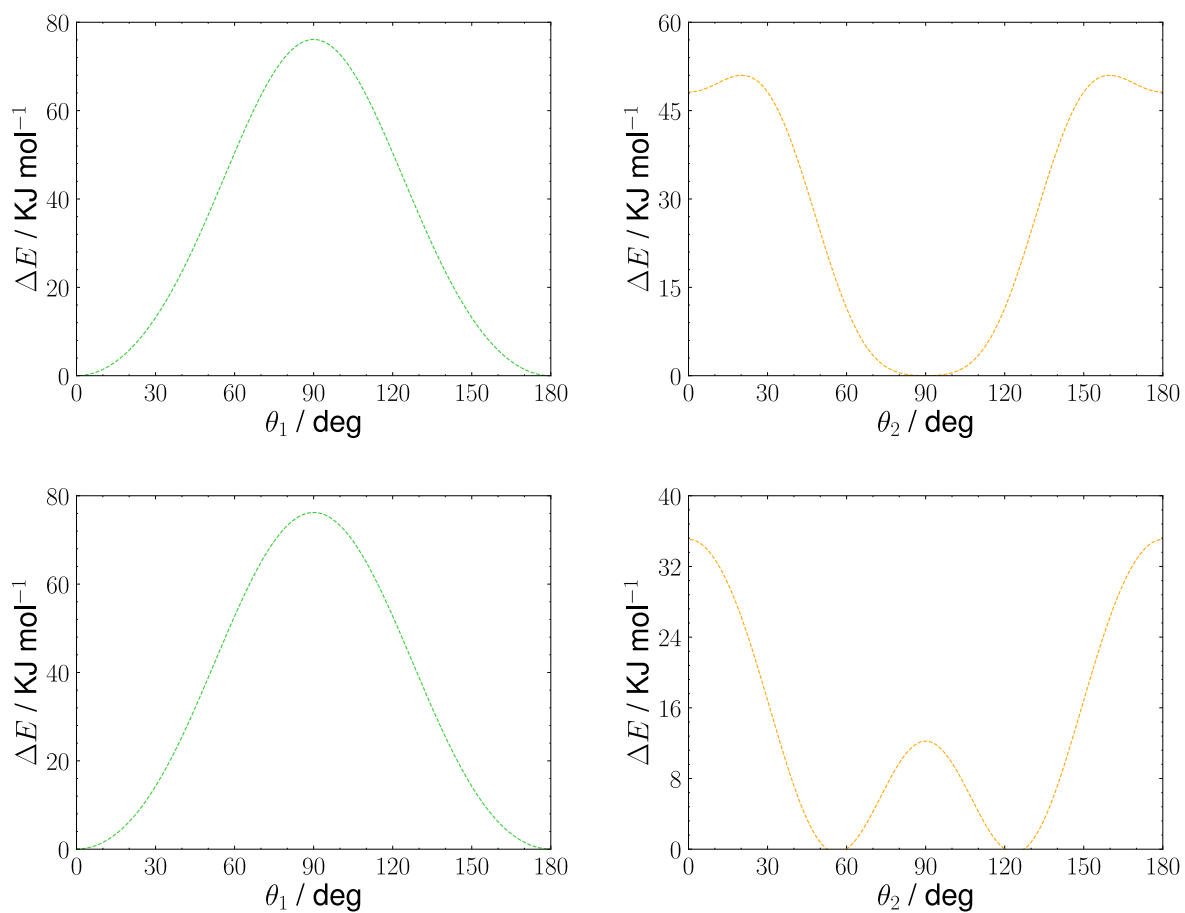
Fig. S4: Fit of QM relaxed scans on S_1 (top) and T_1 (bottom) PESs along θ_1 (left) and θ_2 (right) torsional coordinates for ACPM.
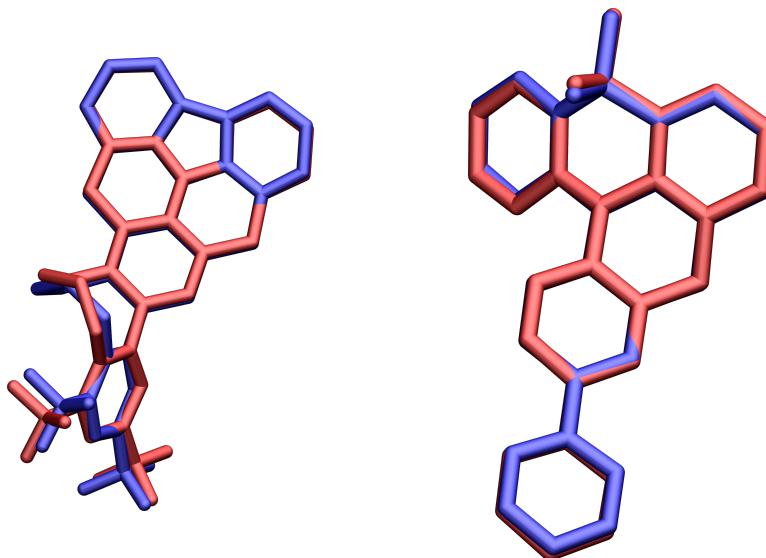
S5 Designed Derivatives

Fig. S5: S_0 (blue) and S_1 (red) minimum geometries for TN4T (left) and ACPM (right) derivatives.

S6 Characterisation of Electronic Transitions

Dye	Functional	E_{HOMO} / eV	E_{LUMO} / eV	E_{S_1} / eV	E_{T_1} / eV	f_{S_1}	ΔE_{ST} / eV
TN4T	Expt.	-5.76	-2.56	3.13	3.03		0.10
TN4T	B3LYP	-5.59	-2.03	3.10	2.78	0.31	0.32
TN4T	M06-2X	-6.85	-1.25	3.97	3.39	0.61	0.58
TN4T	CAM-B3LYP	-6.86	-0.85	4.07	2.94	0.67	1.13
TN4T	PBE0	-5.87	-1.98	3.29	2.80	0.35	0.48
TN4T	ωB97X-D	-7.47	-0.32	4.21	3.11	0.77	1.10
ACPM	Expt.	-5.68	-2.70	3.10	2.80		0.30
ACPM	B3LYP	-5.11	-1.63	2.89	2.88	0.0	0.01
ACPM	M06-2X	-6.41	-0.78	3.88	3.59	0.0	0.29
ACPM	CAM-B3LYP	-6.43	-0.40	4.00	2.97	0.0	1.03
ACPM	PBE0	-5.38	-1.57	3.08	2.98	0.0	0.10
ACPM	ωB97X-D	-7.03	0.13	4.17	3.14	0.0	1.03

Table S2: Characterisation of electronic properties with various density functionals in combination with 6-31G* basis set. B3LYP, CAM-B3LYP and PBE0 calculations include Grimme's dispersion correction.[13]

Dye	E_{S_1} / eV	Assignment	Δr_{S_1} / Å	E_{T_1} / eV	Assignment	Δr_{t_1} / Å
TN4T	3.10	HOMO→LUMO	6.53	2.78	HOMO→LUMO	5.94
ACPM	2.89	HOMO→LUMO	5.99	2.88	HOMO→LUMO	5.99

Table S3: Analysis of electronic transitions to relevant excited states, with assignment and charge transfer metrics. [14]
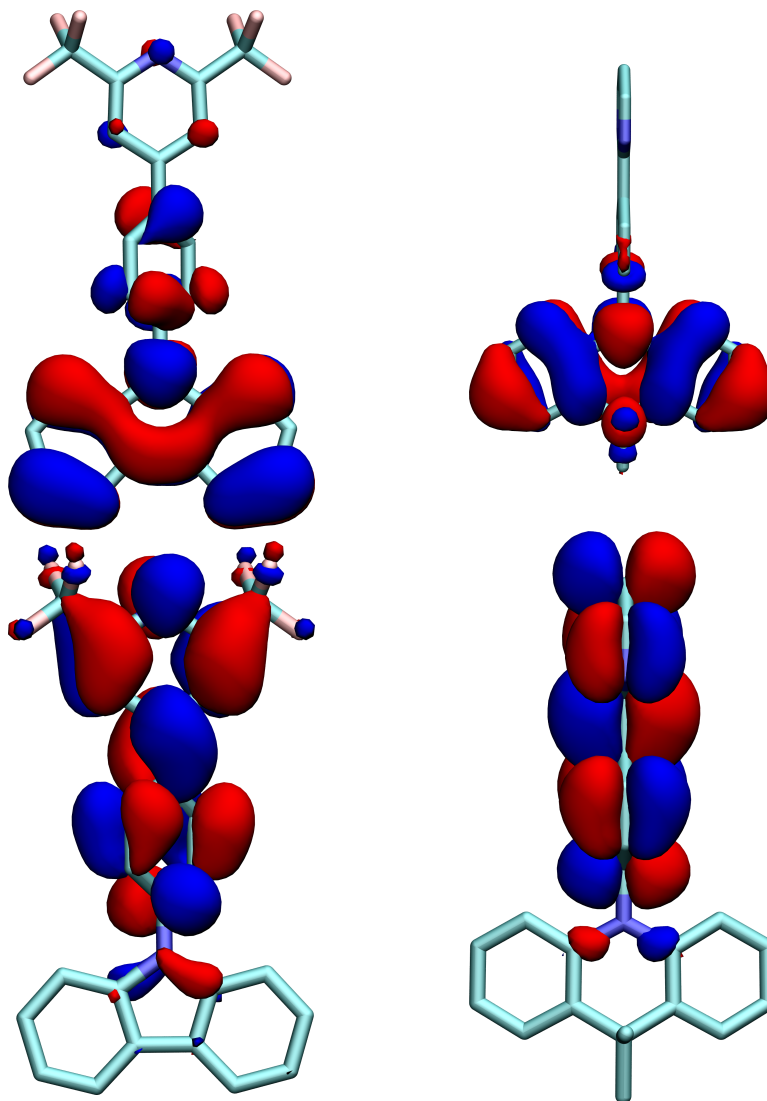

Fig. S6: HOMO (top) and LUMO (bottom) involved in electronic transitions for TN4T (left) and ACPM (right).
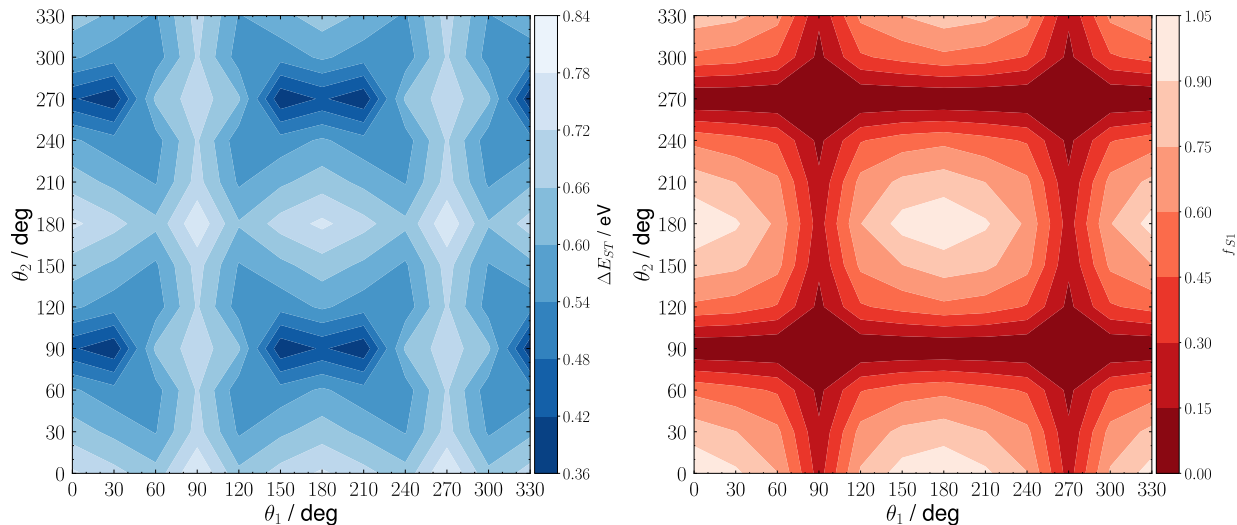
Fig. S7: TDDFT/M06-2X/6-31G* ΔE_{ST} and f_{S_1} as a function of θ_1 and θ_2 for TN4T.

S7 Comparison of TADF quantities for derivatized molecules – T_1 geometry

	θ_1	θ_2	ΔE_{ST} / eV	f_{S_1}	$\langle T_1|\hat{H}_{SO}|S_1\rangle$ / cm^{-1}	k_{rISC} / s^{-1}	k_{ISC} / s^{-1}	k_{em} / s^{-1}
TN4T min	0	44	0.67	0.65	0.53	9.45×10^{-4}	1.73×10^8	1.91×10^9
TN4T planar	0	0	0.84	0.92	0.38	3.56×10^{-7}	6.89×10^7	3.80×10^9
TN4T deriv	−40	0	0.61	0.59	0.27	2.00×10^{-3}	4.82×10^7	1.73×10^9
ACPM min	0	120	0.41	0.28	0.42	2.95	3.06×10^7	$3.01e \times 10^7$
ACPM planar	0	0	0.78	0.57	0.40	1.44×10^{-6}	2.16×10^7	5.55×10^7
ACPM deriv	3	156	0.81	0.79	0.23	1.24×10^{-7}	6.86×10^6	2.78×10^7

Table S4: Comparison of properties and rates relevant for TADF for TN4T and ACPM in their equilibrium geometry, in their planar conformation, and in the conformation forced by the proposed derivatisation. All data refer to the T_1 geometry

References

[S1] R. Kubo and Y. Toyozawa, *Prog. Theor. Phys.*, 1955, **13**, 160–182.

[S2] M. Lax, *J. Chem. Phys.*, 1952, **20**, 1752–1760.

[S3] T. Pizza, *MSc thesis*, Universitá degli studi di Salerno, 2020.

[S4] A. Velardo, R. Borrelli, A. Capobianco, A. Landi and A. Peluso, *J. Phys. Chem. C*, 2019, **123**, 14173–14179.

[S5] Z. Shuai, L. Wang and C. Song, *Theory of Charge Transport in Carbon Electronic Materials*, Springer Press, 2012.

[S6] L. Wang, G. Nan, X. Yang, Q. Peng, Q. Li and Z. Shuai, *Chem. Soc. Rev.*, 2010, **39**, 423–434.

[S7] R. Borrelli and A. Peluso, *WIREs: Comput. Mol. Sci.*, 2013, **3**, 542–559.

[S8] R. Borrelli and A. Peluso, *MolFC: A program for Franck-Condon integrals calculation*, Package available online at `http://www.theochem.unisa.it`.

[S9] R. Borrelli, M. Di Donato and A. Peluso, *Biophys. J.*, 2005, **89**, 830–841.

[S10] A. Peluso, R. Borrelli and A. Capobianco, *J. Phys. Chem. A*, 2013, **117**, 10985–10985.

[S11] H. Sumi and T. Kakitani, *Chem. Phys. Lett.*, 1996, **252**, 85–93.

[S12] T. Renger and R. A. Marcus, *J. Phys. Chem. A*, 2003, **107**, 8404–8419.

[S13] S. Grimme, J. Antony, S. Ehrlich and H. Krieg, *J. Chem. Phys.*, 2010, **132**, 154104.

[S14] C. A. Guido, P. Cortona, B. Mennucci and C. Adamo, *J. Chem. Theory Comput.*, 2013, **9**, 3118–3126.